



Spatial resolution of electron probe X-ray microanalysis on sections of organic (biological) material

E.-R. Krefting^{a,*}, M. Felsmann^{a,1}, A. Recker^{a,2}, B. Feja^{a,3}, H.J. Höhling^a,
R. Reichelt^a, L. Reimer^b

^a*Institut für Medizinische Physik und Biophysik, Westfälische Wilhelms-Universität, Robert-Koch-Str. 31, 48149 Münster, Germany*

^b*Physikalisches Institut, Westfälische Wilhelms-Universität, Wilhelm-Klm-Str. 10, 48149 Münster, Germany*

Received 24 November 1997; received in revised form 17 December 1998

Abstract

A locally enhanced element concentration influences the result of an X-ray microanalysis at a neighbouring position. This influence was investigated for the first time systematically in organic (biological) material using sections of epoxy resin (thickness 0.5–2.5 μm) containing a layer of pure gold. Wavelength and energy dispersive spectrometers were applied to analyse the X-rays generated by 15–35 keV electrons. Characteristic X-rays could be detected up to distances of several μm from the gold layer. For example, for a 2.4 μm thick section and 35 keV electrons the measured apparent gold concentration was above 0.1% (weight% per dry mass) at a distance of 10 μm . Thus, the lateral resolution may be not better than a multiple of the section thickness. The apparent gold concentration at a given distance is proportional to the specimen thickness and increases with increasing electron energy. Monte Carlo simulations confirm the experimental results. The influence of a local enrichment depends on the particular specimen properties (e.g. thickness, density, mean atomic number), the electron energy, and the geometry of the detector with respect to the specimen. © 1999 Elsevier Science B.V. All rights reserved.

PACS: 61.16.Bg; 81.70.J; 87.64.Dz; 87.64.F

Keywords: X-ray microanalysis; Spatial resolution; Section; EPMA; Organic material

* Corresponding author. Tel.: + 49-251-83-55113; fax: + 49-251-83-55144.

E-mail address: kreftin@uni-muenster.de (E.R. Krefting)

¹ Present address: Gatan Inc., 55, 5th street, Hong Lok Yuen, Tai Po, N.T. Hong Kong.

² Present address: Flachglas AG, Haydnstr. 19, D-45884 Gelsenkirchen, Germany.

³ Present address: Biozentrum, Interdepartementale Elektronenmikroskopie, Universität Basel, Klingelbergstr. 70, CH-4056 Basel, Switzerland.

1. Introduction

Electron probe X-ray microanalysis (EPMA) is a well-established method to measure the element concentration of thin biological specimens. The analysed volume of thin specimens is much smaller than that of bulk specimens. It is determined by the thickness of the specimen, the diameter of the electron probe, and some beam broadening in the

specimen. In most cases it is sufficient to take into account that volume, which encloses 90% of the incident electrons [1–3]. However, a minor fraction of electrons is scattered into regions outside this volume and may play an important role when measuring very small element concentrations near a region, where the concentration of these elements is high. Therefore, it is important to know the influence of a local high element concentration on the measurements in its neighbourhood to avoid a misinterpretation of the measurement. EPMA near implants or the analysis of calcium and phosphorus in unmineralized tissue near mineralized tissue (bone, tooth) represent typical examples in biology.

2. Materials and methods

The preparation of the test specimens is shown in Fig. 1a: A layer of gold (Au), 1–2 μm thick, was

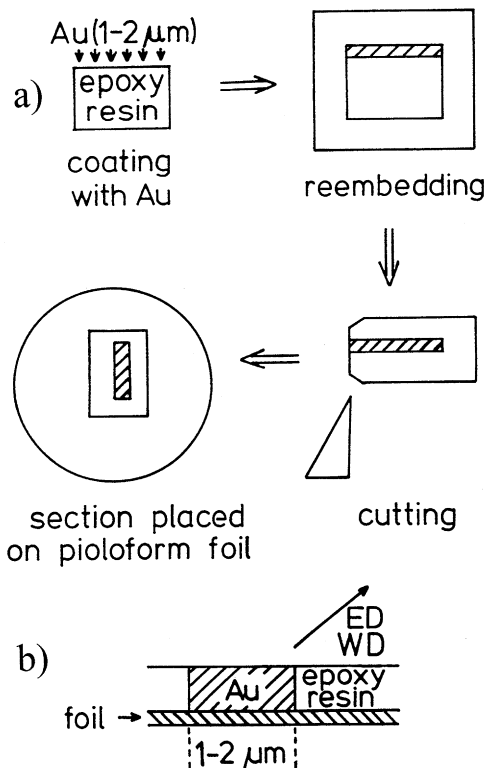


Fig. 1. Preparation (a) and cross-section (b) of the specimens. Sizes are not on scale.

evaporated on the flat surface (size about $1 \times 3 \text{ mm}^2$) of a small piece of epoxy resin [4]. This small piece of epoxy resin with the evaporated Au was reembedded in epoxy resin. After polymerization, sections were cut perpendicular to the Au layer. Their thickness was in the range 0.5–2.5 μm . The sections were transferred onto a thin pioloform foil (about 0.1 μm thick), stretched over an aluminium (Al) tube with an inner diameter of 8 mm. The Al-tubes have been coated with a carbon paint (CCC, PLANO GmbH, Marburg, Germany) to reduce both the backscattering of electrons and the generation of continuum X-rays. Finally, the sections were coated with a thin layer of carbon. Fig. 2 shows a backscattered electron micrograph of a section containing a Au layer. The inhomogeneities in the Au layer result most probably from the sectioning.

The continuum method (Hall-method) was used for quantification [5]. According to this method the concentration c_x of an element x is proportional to the ratio of the characteristic to the continuum X-rays:

$$c_x \sim P_x / (W - W_f), \quad (1)$$

where P_x represents the characteristic counts of element x (background subtracted), W the continuum radiation measured on the specimen, and W_f the continuum radiation measured on the supporting foil.

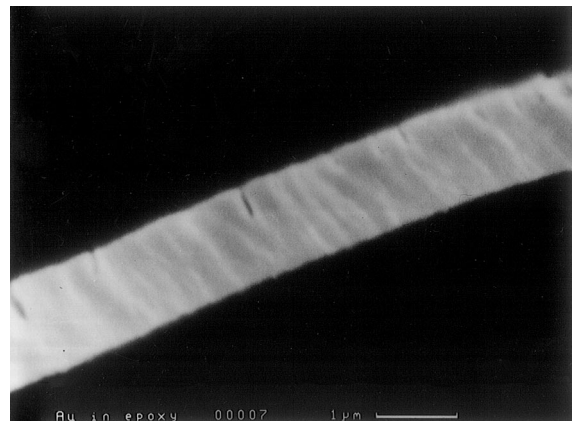


Fig. 2. Backscattered electron micrograph of a 1 μm thick section of epoxy resin with the Au layer. Bar = 1 μm .

A thin layer of Au (about 40 nm thick) evaporated onto a thin pioloform foil was used as standard for the quantification. The concentration c_x is given as wt% per dry mass (g/100 g dry mass) in this paper.

For the analyses the following instruments and conditions were used:

1. *CAMECA microprobe MS46*: Three wavelength dispersive (WD) systems (WD 2: LiF-crystal to measure the Au-L radiation. WD 3 and WD 4: TAP-crystals to measure the Au-M radiation), and an energy dispersive (ED) system (EDAX 505, to measure the continuum radiation). The take-off angle of the X-rays was 18°. Electrons of 15 and 35 keV were used.
2. *CAMSCAN S24*: An ED-system (EDAX 9900, to measure the Au-M, the Au-L, and the continuum radiation). The take-off angle was 30°. Electrons of 20, 27.5, and 35 keV were used.
3. *CAMSCAN S44*: A WD-system (MICROSPEC; LiF-crystal to measure the Au-L radiation), an ED-system (EDAX detector with EDITOR software, to measure the continuum radiation). The take-off angle was 40°. Electrons of 20, 27.5, and 35 keV were used.

All measurements were carried out at normal incidence of the electron probe. The probe current (5 or 10 nA) was measured by a Faraday cup located in the specimen plane. The counting time was 200 s for the ED-system, and 100 or 200 s for the measurements of the characteristic and also of the background radiation with the WD-systems.

The continuum radiation of the foil (W_c) was measured at least on three different positions on the supporting foil near the section.

The thickness of the sections was assumed to be equal to the nominal thickness set at the microtome and verified by the count rate of the continuum radiation.

The continuum radiation W covered the energy range 4.45–7.75 keV and contained no characteristic peaks.

The experimental data were obtained with the different instruments as follows: For the CAMSCAN S24 and S44, the position of the edge of the Au layer was determined on the monitor of the microscope. Seven different series were measured

for each electron energy and section thickness whereby the analysed spots were located at the distances 1, 2, 3,... μm from the Au edge. The mean of the seven measurements is shown in Figs. 4–7.

For the CAMECA microprobe MS46, the position of the Au edge was set according to the intensity of the characteristic X-rays of Au. 3–5 series on different sections were measured for each electron energy and section thickness. The results for the Au-M radiation measured with the spectrometers WD 3 and WD 4 were similar, so that the mean of the corresponding data of these two spectrometers was used if applicable.

To measure the radial distribution $j(r)$ of the electron probe intensity, the electron probe was scanned across a sharp edge of a razor blade or of a silicon chip and the intensity of the transmitted or secondary electrons recorded. $j(r)$ is usually described as

$$j(r) = I/(2\pi\sigma^2) \exp\{-r^2/2\sigma^2\}, \quad (2)$$

where $j(r)$ denotes the intensity of the electron beam at the distance r from its centre, I the total probe current, and σ the variance of the Gauss function. In this case 50% of the incident electrons are contained inside a radius $r = 1.2\sigma$ and 90% inside $r = 2.15\sigma$.

3. Results

The experimental data shown in Figs. 3–6 were selected to demonstrate the characteristic relationships of the apparent concentration of Au to the most important parameters such as distance from the Au layer, section thickness, and electron energy. To reduce the number of graphs only results for Au-M X-rays are shown.

Fig. 3 shows the decrease of the apparent Au concentration with the distance from the Au edge for 35 keV electrons and a section thickness of 2.4 μm . Under these conditions the concentration is still higher than 0.1% at a distance of 10 μm from the Au edge.

For the same electron energy the apparent Au concentration as a function of the section thickness is shown in Fig. 4. The linear fit demonstrates that the apparent concentration is proportional to the

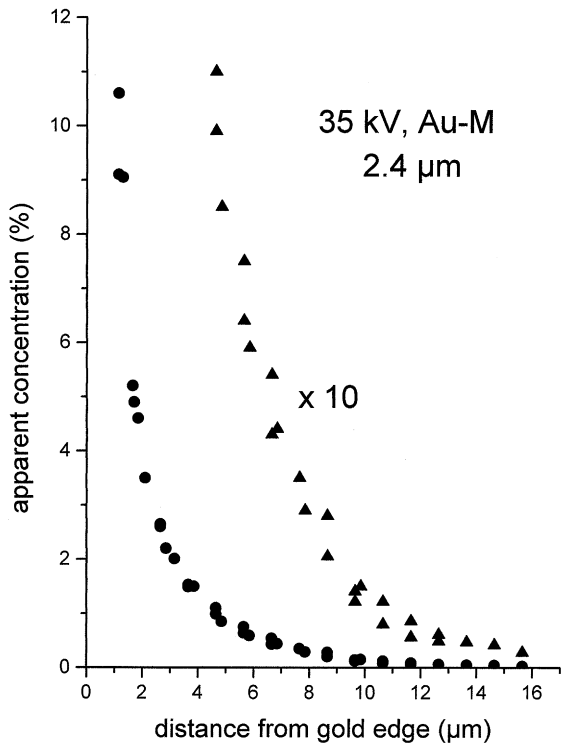


Fig. 3. Apparent (measured) concentration of Au versus the distance from the Au edge. Wavelength dispersive measurement. Operating voltage 35 kV. Au-M radiation. Section thickness 2.4 μm .

section thickness for a given distance from the Au edge at least in the range 2–5 μm .

The distance $R(u)$ from the Au edge where the apparent (measured) Au concentration has fallen to $u\%$ is shown as a function of the specimen thickness in Fig. 5 and of the operating voltage in Fig. 6. The experimental data can be fitted satisfactorily by a linear (Fig. 5) or exponential function (Fig. 6). If we define $R(u = 0.3\%)$ as the lateral resolution, the lateral resolution amounts to a multiple of the section thickness, and its ratio to the section thickness decreases with increasing section thickness (Fig. 5) and increases with increasing electron energy (Fig. 6).

For all measurements shown the analysed spot and the spectrometer were located on the same side of the Au layer (i.e. analysed spot in the draft of the cross section (Fig. 1b) on the right-hand side

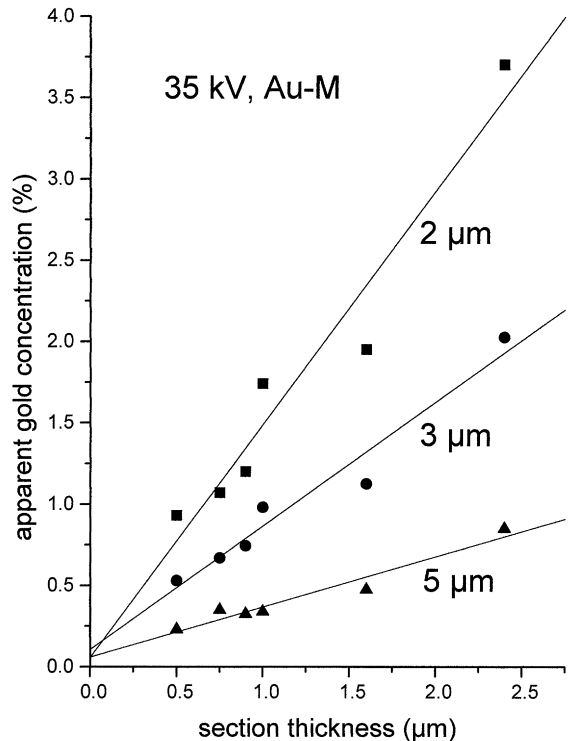


Fig. 4. Apparent (measured) concentration of Au as a function of the section thickness for 2, 3, and 5 μm distance from the Au-edge.

of the Au layer). Measurements with the analysed spots and the spectrometer on opposite sides of the Au layer (i.e. analysed spot in Fig. 1b on the left-hand side of the Au layer) demonstrated, that the absorption of X-rays in the Au layer cannot be neglected.

The results using the Au-L radiation (data not shown) were similar to those shown for Au-M radiation.

For comparison Monte Carlo simulations have been performed [6–8]. The result for Au-M radiation, 35 kV operating voltage, and 1 μm section thickness is shown with corresponding experimental data in Fig. 7. The simulation included 2×10^6 incident electrons.

The radial distribution of the incident beam (Eq. (2)) has been measured for the three microscopes and resulted in $\sigma = (65 \pm 15)$ nm for both the

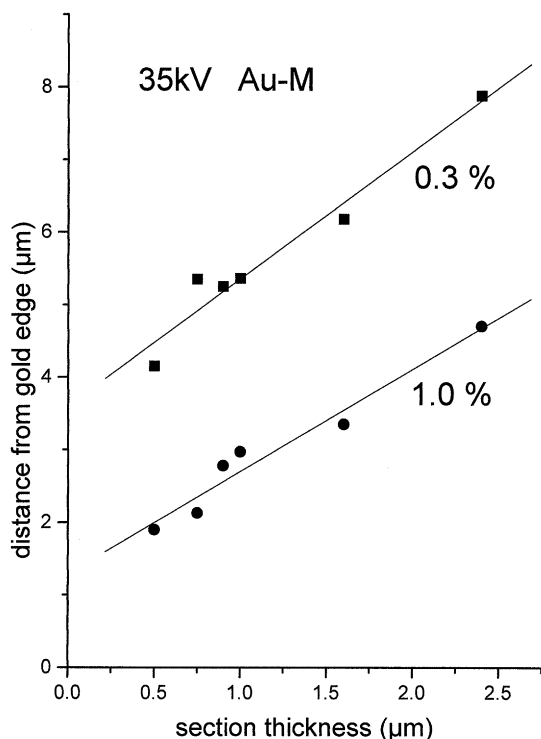


Fig. 5. Distance $R(u)$ from the Au edge where the apparent (measured) Au concentration reaches $u = 0.3\%$ and 1.0% as a function of the section thickness. Linear fit.

CAMSCAN S44 and S24 and $\sigma = (100 \pm 25)$ nm for the CAMECA microprobe.

4. Discussion

For the quantification of our experimental data the continuum method (Hall method) has been applied, which is valid only for thin specimens. A specimen is regarded as thin for EPMA, when the energy loss of the transmitted electrons and the absorption of the generated X-rays is negligible. It is assumed that the energy loss can be neglected when more than 90% of the incident electrons transmit the specimen. This holds for a section of epoxy resin which is thinner than 2 or 5 μm for 20 keV or 35 keV electrons, respectively (the density of epoxy resin is about 1.1 g/cm^3 [4]). The absorption of Au-M and Au-L radiation in the

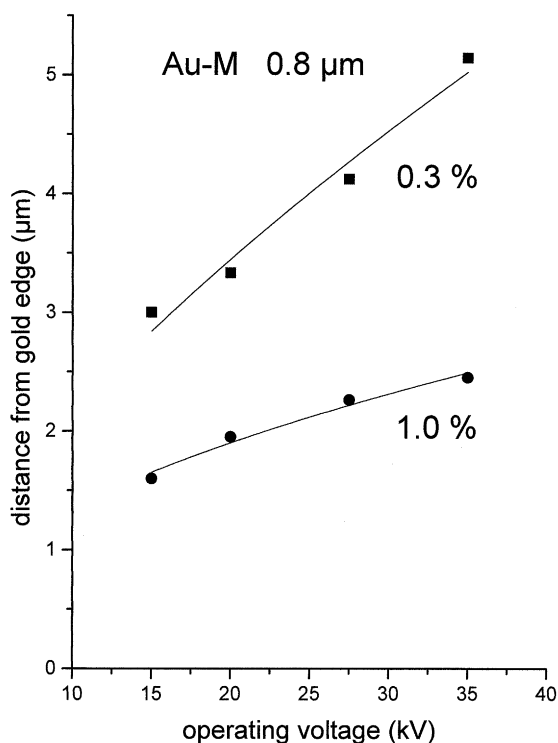


Fig. 6. Distance $R(u)$ from the Au edge where the apparent (measured) Au concentration reaches $u = 0.3\%$ and 1.0% as a function of the operating voltage. Fit by the function aE^b .

epoxy resin can be neglected for sections thinner than $2.5 \mu\text{m}$ as it contributes less than 10%, which compares to the error of the measured element concentrations (s. below). Therefore, the epoxy resin region of all investigated sections can be regarded as thin. In contrast, the range of electrons in Au is only about $0.4 \mu\text{m}$ at 20 kV and $0.8 \mu\text{m}$ at 35 kV assuming a density of gold of 19.3 g/cm^3 [9]. Therefore, the gold layer must be almost regarded as bulk material.

The section thickness was in the range $0.5\text{--}2.5 \mu\text{m}$, which covers that used in many biological applications of EPMA. Sections of epoxy resin (or other materials with similar density) thicker than $2.5 \mu\text{m}$ are too thick to apply the continuum method for elements of interest in biology (e.g. Na and Mg), and in general the spatial resolution is not sufficient for biological applications. For sections thinner than about $0.5 \mu\text{m}$, the

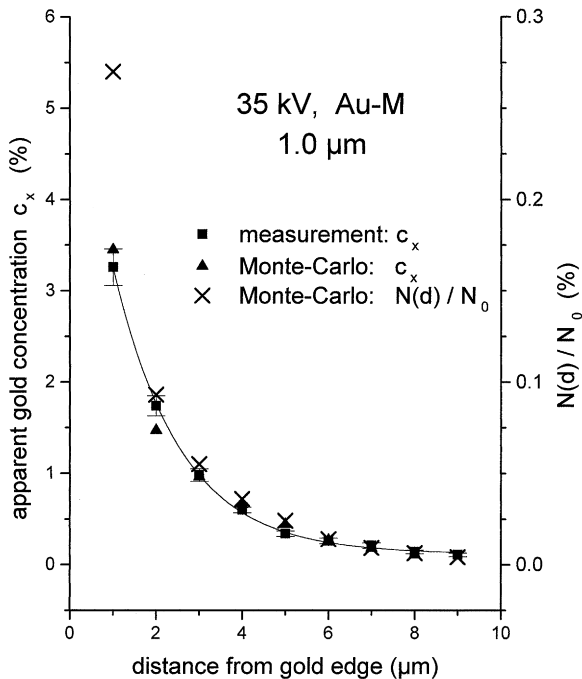


Fig. 7. Fraction $N(d)/N_0$ of electrons reaching the gold layer calculated by Monte-Carlo simulation (crosses), apparent concentration c_x calculated from $N(d)/N_0$ (triangles), and the mean of seven measurements with the standard error of this mean (squares). The experimental data are fitted by an exponential decay $a + b \exp(-cd)$. The coefficient of variation of the Monte Carlo data (statistical error) is about 5%.

intensity of the characteristic X-rays generated in the Au layer is considerably reduced because the electrons transmit the Au layer, so that measurements at distances larger than 1 or 2 μm from the Au edge give no reliable results. Measurements at distances shorter than 1 μm are always unreliable in our experiments (see the following discussion of errors). Thus, sections thinner than 0.5 μm or thicker than 2.5 μm were not used.

Considering the precision of our data, errors may occur in the section thickness, in the distance from the Au edge, and in the calculated (apparent) Au concentration. The evaluation revealed:

1. The error in section thickness amounts to about 0.15 μm according to variations in the continuum radiation.

2. Errors in the distance from the gold edge to the analysed spot may be caused by inaccuracies in the position of the analysed spot, by a drift of the specimen (e.g., due to beam damage), by a drift of the electron probe (e.g. by some charging), and by the roughness of the Au edge (Fig. 2). It is estimated that the inaccuracy in determining the distance from the Au edge may amount to 0.25 μm. This error plays an important role especially for measurements near the Au edge, i.e., for distances less than 1 μm.
3. The error of the element concentrations was determined from the measurements. Usually the element concentration was measured 7 times for a given distance from the Au edge, section thickness, and operating voltage (see Section 2). The mean of these seven values was calculated. The coefficient of variation amounts to $\leq 10\%$ for element concentrations higher than 0.3% (cf. Fig. 7). For element concentrations less than 0.3% the absolute error of the mean amounts to about 0.03%. This standard error of the mean includes all statistical errors, i.e. the statistical error of the measured counts, errors in background subtraction as well as the errors caused by variations of the section thickness and of the distance from the Au edge.

Fig. 4 demonstrates a linear relationship between the apparent Au concentration and the section thickness for a given distance from the Au edge. This linearity can be expected providing that (1) small-angle scattering can be neglected and the electrons are scattered only once, (2) the scattering angle to reach the Au layer (in our measurements about 90°) does not alter significantly across the whole section, and (3) each electron reaching the Au layer generates the same mean number of X-rays. The probability P_1 for electron scattering by a given angle is proportional to the thickness t_s of the specimen. The solid angle Ω to reach the Au layer is also proportional to t_s so that the intensity P of characteristic X-rays generated in the Au layer is proportional to $P_1\Omega$, i.e. to t_s^2 . The intensity $W_s = W - W_f$ of the continuum radiation generated in the section is proportional to t_s , so that the ratio P/W_s (which is proportional to the element concentration c_x , Eq. (1)) is proportional to t_s .

When the thin supporting foil (thickness t_f about $0.1 \mu\text{m}$) is taken into account, the ratio P/W_s is approximately proportional to $t_s + t_f$, because P_1 is proportional to $t_s + t_f$, and Ω and W_s to t_s .

The Monte Carlo simulation revealed the number $N(d)$ of electrons reaching the Au layer at a distance d from the incident beam. $N(d)$ was related to the number N_0 of incident electrons. To calculate $P/(W - W_f)$ (Eq. (1)), $N(d)/N_0$ was multiplied with the number of characteristic X-rays measured on bulk gold, and divided by $W_s = W - W_f$ measured at the given distance. The comparison with our measurements demonstrates a good agreement (Fig. 7). It is of particular interest to point out that the fraction $N(d)/N_0$ of electrons reaching the Au-layer is relatively small, about a factor 20 smaller than the calculated element concentration. For example, at a distance of $3 \mu\text{m}$ $N(d)/N_0$ is about 0.05% while the element concentration is about 1% (Fig. 7).

The spatial (lateral) resolution of EPMA is dependent on the energy E of the incident electrons. Usually, an energy dependence proportional to $1/E$ is proposed [1–3]. However, our data show an increase of $R(u)$ with E (Fig. 6). The reason is that we have used the continuum method for quantification (Eq. (1)). The intensity P_x of the characteristic X-rays generated in the enrichment is proportional to the probability that an electron is scattered towards the Au layer, which is proportional to E^{-2} (Rutherford scattering cross section), multiplied by the probability that characteristic radiation is generated in the thick Au layer, which is proportional to $(U - 1)^{1.65}$ ($U = E/E_c$, $E_c =$ ionization energy) [10]. The intensity of the continuum radiation $W_s = W - W_f$ generated in a thin section is proportional to U^{-1} [11] and the energy dependence of the standard (P/W_s of a thin specimen) is proportional to $\ln U$ [11]. Thus, $c_x \sim (U - 1)^{1.65}/(U \ln U)$, which can be approximated by $0.57 U^{0.45}$ (error less than 5% for $2.5 \leq U \leq 40$). The experimental data were fitted with the function aE^b . The fit resulted in $b = 0.67$ and 0.48 for 0.3% and 1.0%, respectively (Fig. 6), in agreement with the theoretical evaluation.

When other specimens are regarded, the influence of several parameters such as composition, density, and extent of the element enrichment, den-

sity of the section outside of the enrichment, absorption of the X-rays under investigation, section thickness, operating voltage, and tilt angle of the specimen must be taken into account. For example, if the concentration of an element in the enrichment is less than 100%, the apparent concentration is reduced accordingly. In case that the section thickness or the width of the enrichment is significantly smaller than the electron range in the enrichment, the number of generated X-rays and hence the apparent concentration is also reduced.

All measurements presented in this paper were performed at normal incidence of electrons, so that the incident electrons had to be scattered by an angle of about 90° to reach the Au layer. When the specimen is tilted by an angle θ , the scattering angle is about $90^\circ - \theta$ or $90^\circ + \theta$. The differential scattering cross-section depends on the scattering angle. Thus it becomes important for a tilted specimen whether the scattering angle is larger or smaller than 90° and therefore on which side of the local enrichment the analysed spot is located.

Wiesmann et al. [12] have reported measurements at the interface between calcium fluoride (CaF_2) and epoxy resin at 80 kV, section thickness $0.5 \mu\text{m}$ and tilt angle 30° . They have measured an apparent calcium concentration of about 0.015% in a distance of $2 \mu\text{m}$ from the CaF_2 edge. In contrast to our measurements the section thickness was considerably smaller than the range of the electrons in the enrichment, and the specimen was tilted. Thus, a low apparent concentration can be expected. Unfortunately, no quantitative comparison with our results seems feasible.

A typical example in biology is the measurement of Ca in unmineralized soft tissue near bone, dentine, or enamel. As an example, we evaluate the apparent concentration in a freeze-dried unembedded $5 \mu\text{m}$ thick section, 35 kV operating voltage at a distance of $10 \mu\text{m}$ from enamel: The concentration of Ca in enamel is about 40%, the density of enamel (apatite) about 3.1 g/cm^3 , and the density of the freeze dried soft tissue is assumed to equal 0.33 g/cm^3 . The range of 35 keV electrons in enamel is about $5 \mu\text{m}$. For these conditions, the apparent (additional) Ca concentration finally amounts approximately to 0.5%. This apparent concentration is even more than that in other

unmineralized tissues (e.g., about 0.4% in the extracellular matrix of the epiphyseal growth plate cartilage [13]). However, if the section thickness is only 1.5 μm (about $\frac{1}{3}$ of the electron range in apatite), the apparent (additional) Ca concentration is only about 0.09% at a distance of 3 μm , just below the detection limit of Ca for an ED-system [14–16].

Several models are used to describe the electron beam broadening [3]. Williams et al. [3] define the spatial (lateral) resolution of EPMA as the mean of the diameter of the incident probe and the diameter of that area at the bottom of the section, which contains 90% of the electrons. Van Cappellen and Schmitz [2] calculate a cylinder, which encloses 90% of the electrons and thus also about 90% of the X-rays generated in the specimen. The diameter of this cylinder depends on the atomic number Z , density, and thickness of the specimen, and on the energy and beam diameter of the incident electrons. For $Z = 6$, a density 1.1 g/cm^3 (i.e. atomic number and density close to the values of epoxy resin), 35 kV operating voltage, and an incident beam with $\sigma = 65 \text{ nm}$ (Eq. (2)) the diameter R_{cyl} of this cylinder amounts to $R_{\text{cyl}} = 0.36 \mu\text{m}$ or $0.96 \mu\text{m}$ for a section thickness 1 or 2.4 μm , respectively. Using the same conditions, the equation given by Williams et al. [3] reveals a lateral resolution of 0.24 or 0.74 μm , respectively. However, our data demonstrate that with particular specimens this definition of the lateral resolution is not appropriate. If we define as lateral resolution that distance, where the apparent Au-concentration is reduced to 0.3%, we have a resolution of about 5 and 8 μm for the same conditions (Fig. 5), i.e. about a factor 10 worse than given by the models discussed above.

Characteristic X-rays generated by secondary X-ray fluorescence [17] and other spurious X-rays generated outside of the volume of interest [18,19] may also contribute to the measured X-ray spectrum. In our specimens, the generation of characteristic Au X-rays by secondary X-ray fluorescence can be neglected, as the volume of the Au layer is relatively small (compared to the range of X-rays) and no characteristic X-rays are present which can generate Au X-rays by fluorescence. Spurious X-rays generated in the pole piece or in other parts of the SEM were not observed. No characteristic

X-rays are generated in the holder, because it is covered with a carbon paint.

5. Conclusions

In thin as well as in thick sections the lateral resolution of EPMA may be much worse than calculated with published theoretical models [1–3]. The contribution of the surroundings must be taken into account, when the concentration of an element in the neighbourhood of the analysed volume is distinctly higher than within the analysed volume. The resolution improves for lower electron energies.

In ultrathin sections the range of the electrons is significantly larger than the section thickness in all materials, so that the contribution of the neighbourhood is negligible and high-resolution EPMA seems feasible.

Acknowledgements

The authors thank Mrs. U. Malkus for her valuable technical help preparing the sections.

References

- [1] J.I. Goldstein, J.L. Costley, G.W. Lorimer, S.J.B. Reed, *Scanning Electron Microsc.* 1 (1977) 315.
- [2] E. Van Capellen, A. Schmitz, *Ultramicroscopy* 41 (1992) 193.
- [3] D.B. Williams, J.R. Michael, J.L. Goldstein, A.D. Romig Jr., *Ultramicroscopy* 47 (1992) 121.
- [4] A.R. Spurr, *J. Ultrastruct. Res.* 26 (1969) 31.
- [5] T.A. Hall, in: G. Oster (Ed.), *Physical Techniques in Biological Research*, Vol. 1a, Academic Press, New York, 1968, p. 157.
- [6] R. Senkel, *Monte-Carlo Simulationen in der Elektronenmikroskopie*, Thesis, Universität Münster, 1993.
- [7] L. Reimer, R. Senkel, *Optik* 98 (1995) 85.
- [8] L. Reimer, M. Kässens, L. Wiese, *Mikrochim. Acta (Suppl.)* 13 (1996) 485.
- [9] J.R. Young, *J. Appl. Phys.* 27 (1956) 1.
- [10] K.F.J. Heinrich, *Electron Beam X-Ray Microanalysis*, Van Nostrand Reinhold Company, New York, 1981.
- [11] D.F. Kyser, in: J.J. Hren, J.I. Goldstein, D.C. Joy (Eds.), *Introduction to Analytical Electron Microscopy*, Plenum Press, New York, 1979, p. 199.

- [12] H.P. Wiesmann, U. Plate, H.J. Höhling, R.H. Barckhaus, K. Zierold, *Scanning Microsc.* 7 (1993) 711.
- [13] E.-R. Krefting, K. Frentzel, J. Teßarek, H.J. Höhling, *Scanning Microsc.* 7 (1993) 203.
- [14] J.I. Goldstein, in: J.J. Hren, J.I. Goldstein, D.C. Joy (Eds.), *Introduction to Analytical Electron Microscopy*, Plenum Press, New York, 1979, p. 83.
- [15] E.R. Krefting, U. Scholz, W. Zidek, *Beitr. Elektronenmikroskop. Direktabb. Oberfl.* 23 (1990) 385.
- [16] J.I. Goldstein, D.E. Newbury, P. Echlin, D.C. Joy, A.D. Romig Jr., C.E. Lyman, C. Fiori, E. Lifshin, *Scanning Electron Microscopy and X-Ray Microanalysis*, second ed., Plenum Press, New York, 1992.
- [17] I.M. Anderson, J. Bentley, C.B. Carter, *Ultramicroscopy* 68 (1997) 77.
- [18] Y.H. Li, Z. Chen, M.H. Loretto, *J. Microsc.* 170 (1993) 259.
- [19] R.F. Egerton, S.C. Cheng, *Ultramicroscopy* 55 (1994) 43.